Science of the Total Environment 851 (2022) 157926

Contents lists available at ScienceDirect

Science of the Total Environment

journal homepage: www.elsevier.com/locate/scitotenv

Long-term soil water limitation and previous tree vigor drive local variability of drought-induced crown dieback in *Fagus sylvatica*

S. Klesse [a,*], T. Wohlgemuth [a], K. Meusburger [b], Y. Vitasse [a], G. von Arx [a,c], M. Lévesque [d], A. Neycken [d], S. Braun [e], V. Dubach [f], A. Gessler [a,d], C. Ginzler [g], M.M. Gossner [d,f], F. Hagedorn [b], V. Queloz [f], E. Samblás Vives [a,h], A. Rigling [a,d], E.R. Frei [a,i,j]

[a] Forest Dynamics, Swiss Federal Institute for Forest, Snow and Landscape Research WSL, 8903 Birmensdorf, Switzerland
[b] Forest Soils and Biogeochemistry, Swiss Federal Institute for Forest, Snow and Landscape Research WSL, 8903 Birmensdorf, Switzerland
[c] Oeschger Centre for Climate Change Research, University of Bern, Bern, Switzerland
[d] Institute of Terrestrial Ecosystems, ETH Zurich, 8092 Zurich, Switzerland
[e] Institute for Applied Plant Biology AG, Witterswil, Switzerland
[f] Forest Health & Biotic Interactions, Swiss Federal Institute for Forest, Snow and Landscape Research WSL, 8903 Birmensdorf, Switzerland
[g] Land Change Science, Swiss Federal Institute for Forest, Snow and Landscape Research WSL, 8903 Birmensdorf, Switzerland
[h] Autonomous University of Barcelona (UAB), 08193 Cerdanyola del Valles, Spain
[i] Alpine Environment and Natural Hazards, WSL Institute for Snow and Avalanche Research SLF, 7260 Davos Dorf, Switzerland
[j] Climate Change and Extremes in Alpine Regions Research Centre CERC, 7260 Davos Dorf, Switzerland

HIGHLIGHTS

- Across stands, crown damage severity increased with decreasing water availability.
- Trees growing in drier sites were shorter and their growth was more sensitive to climate.
- Within stands, slower-growing trees under increased competition showed more damage.
- We identified previous tree vigor as a driver of damage severity within and across stands.

GRAPHICAL ABSTRACT

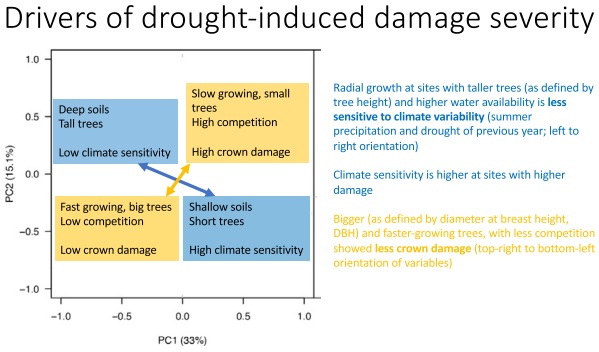

ARTICLE INFO

Editor: Elena Paoletti

Keywords:
Tree rings
Competition
Tree size
Climate sensitivity
European beech
Crown damage

ABSTRACT

Ongoing climate warming is increasing evapotranspiration, a process that reduces plant-available water and aggravates the impact of extreme droughts during the growing season. Such an exceptional hot drought occurred in Central Europe in 2018 and caused widespread defoliation in mid-summer in European beech (*Fagus sylvatica* L.) forests.
Here, we recorded crown damage in 2021 in nine mature even-aged beech-dominated stands in northwestern Switzerland along a crown damage severity gradient (low, medium, high) and analyzed tree-ring widths of 21 mature trees per stand. We aimed at identifying predisposing factors responsible for differences in crown damage across and within stands such as tree growth characteristics (average growth rates and year-to-year variability) and site-level variables (mean canopy height, soil properties).
We found that stand-level crown damage severity was strongly related to soil water availability, inferred from tree canopy height and plant available soil water storage capacity (AWC). Trees were shorter in drier stands, had higher year-to-year variability in radial growth, and showed higher growth sensitivity to moisture conditions of previous late

* Corresponding author.
E-mail address: stefan.klesse@wsl.ch (S. Klesse).

http://dx.doi.org/10.1016/j.scitotenv.2022.157926
Received 20 May 2022; Received in revised form 3 August 2022; Accepted 5 August 2022
Available online 17 August 2022

summer than trees growing on soils with sufficient AWC, indicating that radial growth in these forests is principally limited by soil water availability. Within-stand variation of post-drought crown damage corresponded to growth rate and tree size (diameter at breast height, DBH), i.e., smaller and slower-growing trees that face more competition, were associated with increased crown damage after the 2018 drought. These findings point to tree vigor before the extreme 2018 drought (long-term relative growth rate) as an important driver of damage severity within and across stands. Our results suggest that European beech is less likely to be able to cope with future climate change-induced extreme droughts on shallow soils with limited water retention capacity.

1. Introduction

Global warming is projected to change not only mean climate conditions but also climate variability, leading to more frequent and intense climate extremes such as heatwaves and droughts (Cook et al., 2014; IPCC, 2021). This poses major challenges to forests, which are major contributors to the land carbon sink (Pan et al., 2011), and the plethora of ecosystem services they provide, including biodiversity (Trumbore et al., 2015). In addition to negatively impacting forest carbon sequestration (Anderegg et al., 2013; Ciais et al., 2005; Trotsiuk et al., 2020), extreme droughts have been identified as the primary causes of widespread tree mortality across the globe (Allen et al., 2015, 2010), further reducing the global warming mitigation potential of forests (Anderegg et al., 2020; Bastin et al., 2019).

Premature leaf senescence in temperate broadleaved trees has been shown to occur under extreme droughts and to correlate with heat and water availability in early summer (Bigler and Vitasse, 2021) when radial growth rates are highest (Etzold et al., 2022). Premature leaf senescence could be viewed as a mechanism preventing further water loss from leaves under intense droughts, allowing trees to recover the following year (Bréda et al., 2006). Conversely, leaf senescence could also occur simultaneously with or as a direct consequence of irreversible hydraulic failure due to vessel cavitation in branches (Walthert et al., 2021). In the latter case, premature leaf senescence and partial dieback of canopies and stems may be early indicators of subsequent drought-induced tree mortality (Bréda et al., 2006; Jump et al., 2017; Wohlgemuth et al., 2020).

In the long line of temperature record-breaking years of the 2010s, and following an already prolonged period of severe large-scale soil water deficits (Moravec et al., 2021, Fig. S1), another extreme drought hit Central Europe in the summer of 2018. With average growing season temperatures (April–October) in Germany, Switzerland, and Austria >3.3 °C above the 1961–1990 climate norm, and precipitation well below average, the impacts on forest ecosystems were massive (Baltensweiler et al., 2020; Brun et al., 2020; Schuldt et al., 2020; Sturm et al., 2022). In particular, European beech (*Fagus sylvatica* L.), the most abundant and dominant broadleaved tree species in Central Europe, showed widespread leaf discoloration and premature leaf shedding as early as July (Rohner et al., 2021; Schuldt et al., 2020; Wohlgemuth et al., 2020). Following the abnormal premature leaf senescence in 2018, partial dieback of canopies and higher rates of mortality in beech forests have been observed throughout Central Europe, albeit with high spatial heterogeneity (Frei et al., 2022; Meyer et al., 2022). Thus, the question arises as to what factors caused such heterogeneous crown damage and tree mortality in regions with largely identical meteorological drought conditions.

There is evidence that large (trunk diameter) and tall (tree height) trees are among the most-affected trees within stands during droughts (Bennett et al., 2015; Grote et al., 2016; Stovall et al., 2019). This is often explained by increased inherent vulnerability to hydraulic stress and cavitation (McDowell and Allen, 2015) and by the fact that exposed crowns of the tallest trees within a stand experience higher radiation and atmospheric evaporative demand (Roberts et al., 1990). Alternatively, it has been discussed that shallower rooting depth could make smaller trees more susceptible to the processes of hydraulic failure and carbon starvation (McDowell et al., 2013; Ripullone et al., 2020). Across stands, drought mortality risk increases with higher competitive pressure (Knapp et al., 2021; Rigling et al., 2013; Young et al., 2017) and sensitivity to drought variability (Keen et al., 2022), which in turn is increased in stands with lower soil water availability (Fritts et al., 1965). It is generally accepted that background tree mortality, i.e. mortality that is not attributed to a specific event, is largely a function of tree size and relative growth rates (Cailleret et al., 2016; Gillner et al., 2013; Hülsmann et al., 2018). However, covariation between individual tree traits mentioned above within sites and across sites with varying environmental conditions (e.g., average water availability) can often confound mortality risk predictions (Trugman et al., 2021).

Here, we investigated nine mature beech stands in northwestern Switzerland along a stand-level crown damage severity gradient observed following the exceptional 2018 drought (low, medium, heavy). Within each stand, we assessed crown damage and analyzed tree-ring widths of 21 mature trees that presented various degrees of crown damage after the 2018 drought. We aimed to identify predisposing factors that could explain within- and across-stand variability in crown damage, such as plant-available soil water storage capacity (AWC), tree size, competition, and tree vigor (as defined by long-term pre-event growth rate, Buchman et al., 1983; Monserud and Sterba, 1999).

Specifically, we addressed the following hypotheses:

H1. Because hydraulic limitation theory (Ryan and Yoder, 1997) posits that canopy height is lower for trees of the same species and age on resource-limited sites, we expect stand-level crown damage to be higher on sites with lower water availability, reflected by lower canopy heights and lower AWC.

H2. Stand-level damage is proportional to long-term climate sensitivity of trees derived from tree ring-width time series, i.e., crown damage is more severe in stands with higher interannual tree growth variability.

H3. Within-stand damage differences are related to small-scale resource limitation and tree growth vigor, i.e., trees experiencing higher competition and/or smaller (lower social position) and slow-growing trees show higher crown damage.

2. Material and methods

2.1. Study area

The study area was located in the Ajoie region, Canton du Jura, in northwestern Switzerland (47.48 °N, 7.08 °E) at 450–540 m a.s.l. on bedrock mainly consisting of limestone. During the 1981–2010 period mean annual precipitation was 1050 mm and mean annual temperature was 9.5 °C (Swiss Federal Office of Meteorology and Climatology). Forests in the region are dominated by European beech mixed with sessile and pedunculate oaks (*Quercus petraea* (Matt.) Liebl. and *Quercus robur* L., respectively), European ash (*Fraxinus excelsior* L.) and silver fir (*Abies alba* Mill.). We investigated nine 100–150 years-old stands that showed different stand-level crown damage classes (low, medium, high) following the 2018 drought, with each damage class replicated three times (stand IDs: 1x, 2x, 3x, where x is L(ow), M(edium), or H(igh), Table 1, Fig. 1). The stand-level damage classes referred to the classification of the cantonal forest authority who defined stand damage in summer 2019 according to the proportion of trees with strong crown damage, with 10%, 50%, or 75% of trees within a stand showing multiple dead branches. These semi-quantitative field assessments were confirmed using Normalized Difference Water Index (NDWI) and Normalized Difference Vegetation Index (NDVI) from

Table 1
Site characteristics, characteristics of the sampled trees (mean ± standard deviation), and detrended basal area increment (BAI) chronology statistics (1931–2017) of the nine forest stands. Soil depth: mean depth from soil probes taken next to each sampled tree; AWC: plant-available soil water storage capacity derived from soil profile; Canopy height: mean tree height derived from vegetation height model; DBH: tree diameter at breast height; Age: tree age derived from ring width time series; TCL 2021: mean total crown biomass loss in 2021 (%); ACF: first-order auto-correlation of spline-detrended site chronology; SD: standard deviation of spline-detrended site chronology, rbar: mean inter-series correlation of individual spline-detrended time series.

Stand	Soil depth (cm)	AWC (mm)	Canopy height (m)	DBH (cm)	Age (years)	TCL 2021 (%)	# Trees TCL ≥ 50%	# Trees TCL ≥ 90%	ACF	SD	rbar
1L	87	302	32.5	51.9 ± 7.3	156 ± 7	23 ± 12	1	0	0.27	0.20	0.49
1M	28	35	24.8	41.7 ± 6.7	103 ± 7	55 ± 39	10	7	0.09	0.28	0.68
1H	41	57	28.2	47.9 ± 7.0	136 ± 4	57 ± 32	10	5	0.33	0.28	0.67
2L	94	223	38.4	52.8 ± 5.6	143 ± 10	21 ± 11	0	0	0.12	0.22	0.48
2M	89	297	36.2	53.5 ± 8.9	172 ± 4	53 ± 26	11	3	0.08	0.23	0.48
2H	49	195	33.1	51.5 ± 6.6	168 ± 6	67 ± 32	13	9	0.23	0.27	0.62
3L	40	50	30.2	50.6 ± 10.1	115 ± 10	27 ± 31	3	2	0.13	0.24	0.50
3M	57	119	27.6	48.5 ± 7.8	129 ± 6	41 ± 32	6	3	0.25	0.30	0.66
3H	37	50	24.8	43.3 ± 6.5	140 ± 10	61 ± 35	11	7	0.37	0.29	0.65

Sentinel-2 images (Fig. S2; Copernicus Open Access Hub, 2022; Gao, 1996), where all raster tiles (resolution: 20 m) within a circular radius of 100 m around the plot center were averaged, excluding tiles without forest cover.

All stands were situated within an area of 20 km^2 (maximum distance between stands = 9 km). Within each stand, we selected 21 mature beech trees with DBH >30 cm. The 21 trees were grouped in triplets. Each triplet was chosen to contain three trees of similar size with varying degrees of crown damage (low, medium, high) growing in proximity to each other, i.e., presumably sharing similar microhabitat conditions. All trees of a stand grew within an area of 1600–5000 m^2 (mean: 3055 m^2, standard deviation: 995 m^2).

2.2. Stand-level environmental data

2.2.1. Climate data

We used monthly climate data of mean daily minimum and maximum air temperature (T_{min}, T_{max}), and precipitation sums (PPT) beginning in 1930 that were interpolated to a spatial resolution of 100 m with the DAYMET method (Thornton et al., 1997) based on MeteoSwiss weather stations (Swiss Federal Office of Meteorology and Climatology). Calculation of Standardized Precipitation-Evapotranspiration Index (SPEI) was performed using the Hargreaves formula (R package *SPEI*, Beguería and Vicente-Serrano, 2017).

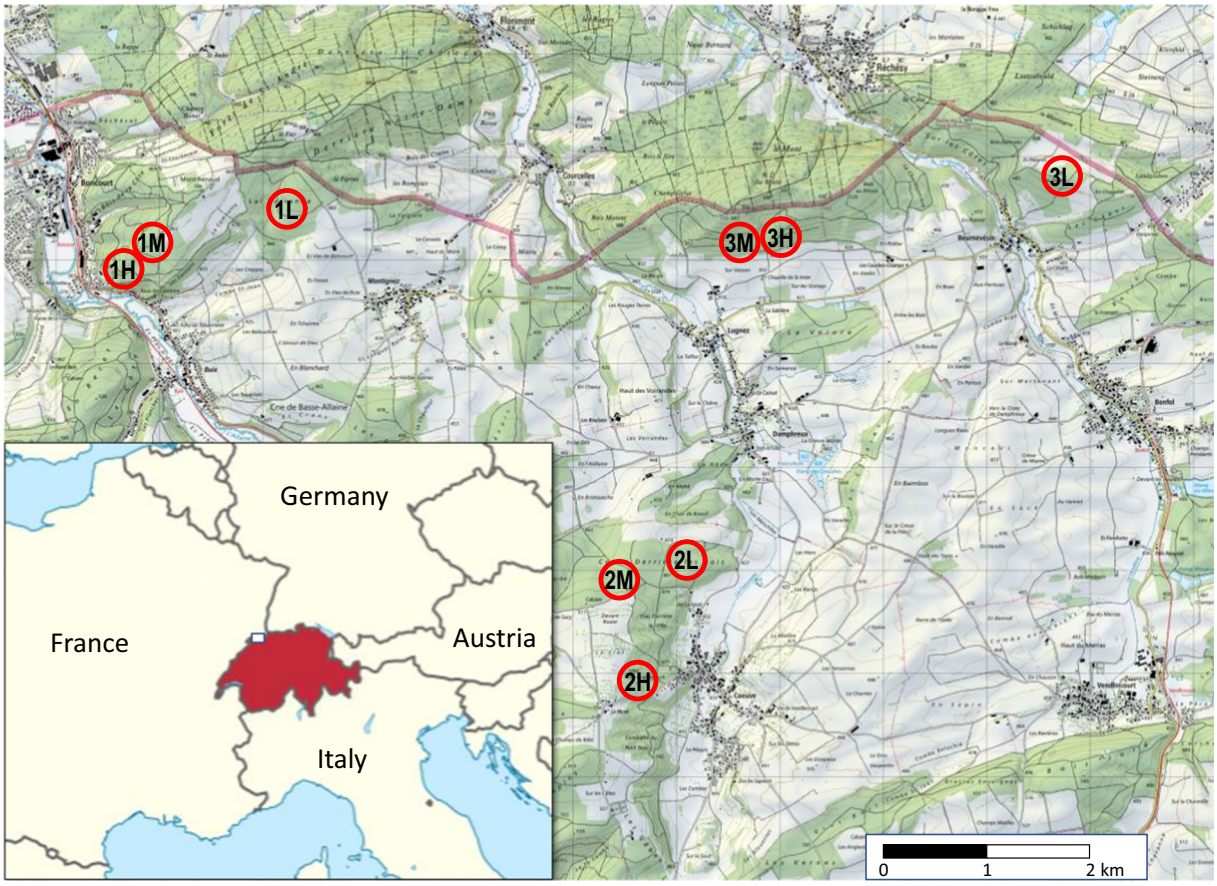

Fig. 1. Ajoie region in Switzerland (white rectangle in red area) with the nine studied stands showing low (L), medium (M), and high (H) crown damage. © Data: swisstopo; map.geo.admin.ch.

2.2.2. Mast index

Massive fruit production, known as mast, shifts carbon allocation away from secondary growth, resulting in narrower tree rings in mast years (Braun et al., 2017; Hacket-Pain et al., 2018; Nussbaumer et al., 2021). To account for this effect, we used the pollen-derived mast index for beech from Basel 40 km away from our study region (1971–2016, Swiss Federal Office of Meteorology and Climatology; Ascoli et al., 2017). The index ranges from 1 to 5, indicating very low to very high pollen production.

2.2.3. Soil data and AWC calculation

At each stand, we dug a soil profile down to the bedrock, to determine texture, bulk density, organic carbon content, gravel content, and thickness of each soil horizon. Based on this layered soil information, we predicted the AWC based on the pedotransfer function of Puhlmann and von Wilpert (2011). Time series of monthly soil matric potential (SMP) were simulated with the soil vegetation atmosphere transport model LWFBrook90 (Hammel et al., 2001) following Schmidt-Walter et al. (2020). We used daily meteorological data (same product as mentioned above with daily resolution) as forcing data for simulating i) the water fluxes through the rooted soil layers and ii) the relative change of leaf area index over the year with the R package *vegperiod* version 0.3.1 (Nuske, 2021). Due to the lack of calibration data, we adopted model parameters from a nearby beech site with comparable soil properties and matric potential measurements (Meusburger et al., 2022). Additionally, to validate the individual point measurement from the soil profile, we determined the soil depth next to each tree with a 160 cm long metal probe.

2.2.4. Canopy height

Coordinates of each tree were recorded using a Trimble GeoXH 6000 DGNSS handheld GPS receiver (Trimble Navigation Limited, Sunnyvale, CA, USA). Post-processed data achieved a horizontal precision of 0.1–2 m. Based on these coordinates, tree heights were determined from a vegetation height model, which was derived from airborne laser scanning data from 2019 with a resolution of 1 × 1 m. The maximum height within a circular buffer area with a radius of the GPS precision plus 5 m was used as the tree height. We used the mean of the individual tree heights (canopy height) as a proxy for site fertility and water availability. Remotely sensed tree heights were validated against tree heights of five trees per site that were measured in the field with a Vertex IV (Haglöf, Sweden; $r = 0.80$). Generally, the remotely sensed tree heights did not vary a lot within a site (range 2–4 m).

2.3. Tree-level data

2.3.1. Crown damage assessment

In June 2020 and 2021 we assessed crown damage of each of our target trees. We recorded crown transparency (CT) of living branches (Eichhorn et al., 2020) and the volume percentage of dead branches (%DB). %DB was assessed as the volume proportion of dead branches (including lost branches) relative to the volume of the total potential crown of the healthy tree, thereby excluding naturally dying branches in the shaded part of the crown (Dobbertin et al., 2016). Based on these two field assessments we calculated the percentage of total crown biomass loss (TCL) as $TCL = \%DB + (100 - \%DB) * CT/100$ (Frei et al., 2022). The crown damage data of 2020 and 2021 were quite similar (Fig. S3, $r = 0.84$), and only small differences were found in preliminary analyses. We thus only present analyses and results with crown damage data of 2021 that better reflect lasting crown damages.

2.3.2. Competition

Around each of our target trees *i*, we recorded DBH and distance to neighboring trees *j* to calculate the competition index (CI) following Hegyi (1974):

$$CI_i = \sum_{j=1}^{n} \frac{DBH_j / DBH_i}{Distance_{ij}}$$

A higher CI value indicates higher competitive pressure on a given target tree. We included neighboring trees up to a distance of 13 m and with a minimum DBH of 20 cm to reduce assessment time in the field.

2.3.3. Tree-ring data

In late summer 2020, we collected two 5 mm increment cores at breast height from opposite sides of the stem and perpendicular to the slope of each of the 21 trees per stand. Core surfaces were prepared with a sledge microtome (Gärtner and Nievergelt, 2010) and subsequently filled with chalk to enhance the visibility of tree-ring boundaries. Images were taken with a digital camera (Canon EOS 5DSR and a 100 mm macro lens, *Skippy - WSL*, 2022) at a resolution of 5950 dpi and ring widths were subsequently measured in CooRecorder v8.9 (Cybis Electronics, Sweden). To relate crown damage to recent growth rates, we transformed raw ring widths to absolute growth rates (basal area increment, BAI) starting from the outside using the DBH measured in 2020 (R Package *dplR*, Bunn et al., 2019). To investigate the effect of size-independent growth rate, we detrended BAI based on a stand-level size-growth relationship (similar to regional curve detrending, Briffa and Melvin, 2011). First, we averaged individual BAI measurements of both cores to a tree-level mean BAI. Then, we ran for each stand a linear mixed-effects model predicting log-transformed BAI as a function of log-transformed DBH of the previous year, including the individual trees as random intercepts (R package *lme4*, Bates et al., 2015). The observed BAI divided by the predicted BAI (using only the fixed effect, and back-transformed to the original unit) yielded the size-detrended BAI (BAIstd).

For the climate-growth response analysis, we detrended the BAI time series with a cubic smoothing spline with a 50% frequency response cut-off at 30 years ("30-year spline") to reduce possible influences of stand dynamics (past management, disturbances) on the growth time series. We averaged the individual BAIstd series with a bi-weight robust mean within each stand (nine site chronologies each including 21 trees), and for each stand-level damage class (three damage-level chronologies each including 63 trees), as well as for the whole study region (one regional chronology using all 189 trees). For both individually spline-detrended time series and site-level chronologies we calculated first-order auto-correlation and standard deviation (sd) over the periods 1931–2017 and 1971–2016. The longer period was defined by the length of the climate data, and the shorter by the mast index data. We omitted the last two years (2018 and 2019) of the chronologies from the analysis because we were interested in predisposing factors explaining post-drought effects.

2.4. Statistical analysis

2.4.1. Climate growth analysis

To identify the climatic influence on interannual tree growth variability in our study area, we calculated Spearman's rank correlations between the regional chronology and mean monthly maximum temperatures, monthly precipitation sums, SPEI, and regional mean soil matric potential over the 1931–2017 period. We conducted the correlation analysis with all possible seasonal aggregation periods from 1 to 12 months and season end months from previous year January to current year October to find the season with the highest correlation (Klesse et al., 2018a). We used common nomenclature for target seasons from SPEI, i.e., "Climate Variable X"$_3$ of August or "Climate Variable X" of August$_3$ means a three months-long season ending in August. All climate time series were also detrended with a 30-year spline using subtraction instead of division (Klesse et al., 2018a).

After the correlation analysis, we chose two independent seasons with the highest correlations for each climate variable with a season length buffer of ±1 and the end month of ±1 to search for the best predictive model in a multiple regression framework. Early exploratory analyses revealed the benefit of including short-term (season length 1–2 months) summer precipitation into the model selection procedure. We restricted the number of maximum predictors to five (plus the intercept). Model selection was performed using the Bayesian Information Criterion (BIC) using *dredge* in the R package *MuMIn* (Bartoń, 2018). We additionally performed

the analysis over the 1971–2016 period including mast index as an additional predictor.

Based on the hypothesis that climate sensitivity should be higher at sites with higher stand-level damage (H2), we used the predictors of the best regional models (1931–2017, 1971–2016) in regressions with the damage-class aggregated and site-level chronologies. We tested for significant differences between climate sensitivity and the three damage classes by adding an interaction term of a target climate variable and damage class. Further, we investigated whether spline-detrended stand-level chronologies show higher year-to-year variability (i.e., higher general climate sensitivity during the 1971–2016 period) at sites with lower AWC, soil depth, and mean canopy height with linear regressions.

In addition, we tested whether the standard deviation of the spline detrended tree-level time series (1971–2016) was dependent on tree size (DBH), mean BAI (2008–2017), and the stand-level variables canopy height, AWC, or soil depth, in a linear mixed-effects model. Lastly, we applied a mixed-effects model to test the effect of competition index (CI) on mean BAI (2008–2017), including the three stand-level water availability variables and DBH as predictors. In both models stand ID was included as a random intercept and we performed model selection based on BIC as described above.

2.4.2. Generalized linear mixed-effects models of crown damage

We used generalized linear mixed-effects models with a logit link and binomial error distribution to investigate the influence of tree-individual parameters on crown damage (R package *lme4,* Bates et al., 2015). We modeled the fixed effects of DBH, mean absolute growth rate (BAI) and size-independent mean growth rate (BAIstd) during the last 10 years before the drought (2008–2017), growth variability (standard deviation, SD) over the 1971–2016 period, and competition index on total crown biomass loss (TCL/100) and crown transparency (CT/100) including the stand-level variables canopy height, soil depth, and AWC as predictors, and including stand ID as random intercept. We also tested a random intercept with the triplet identity nested in site, but this was found to be uninformative and was therefore discarded. All variables included in the models were normalized beforehand. Similar to the climate-growth multiple regression analysis, we performed model selection based on BIC.

2.4.3. Principal component analysis

Principal component analysis (PCA) was applied as an additional means to visualize patterns of common variability among the various above-mentioned tree- and stand-level variables.

For the tree-level variables, we used DBH, mean absolute growth rate (BAI), size-independent growth rate (BAIstd, 2008–2017), CI, CT, and TCL of 2021. The site-level variables included AWC, canopy height, and soil depth. The standard deviation over the 1971–2016 period and coefficients to SPEI_Aug6, SPEI_pSep4, and PPT_Jun1 (derived from the climate-growth multiple regression analysis over the 1971–2016 period, see section climate growth analysis above) were included at both tree and site level. All variables were normalized before the PCA. All analyses were performed in R v4.1.2 (R Core Team, 2021).

3. Results

3.1. Stand and tree growth characteristics

The three stand-level variables describing water availability (soil depth, canopy height, and AWC) were strongly positively correlated to each other (all $r \geq 0.81, p < 0.01$). All three variables were negatively related to stand-level damage, although correlations were not significant (Spearman's rho = 0.42 for canopy height and soil depth, and 0.26 for AWC; all $p > 0.1$). Within stands, trees exhibited a strong coherence in interannual growth variability (rbar > 0.5, Table 1) that was also reflected in a high average correlation between the nine stands (rbar = 0.75). Common narrow rings were observed in 1976, 2011, and 2017, and across all stands, 2007 stood out as a wide ring (large BAI in Fig. 2). In most stands, a notable declining trend in radial growth has occurred during the last decade, which was more pronounced in trees with higher crown damage. The ring width in 2018 was not abnormally small (ring-width index = 0.89, Fig. S4), however, in many trees showing strong crown damage, the 2019 ring was extremely small (see Fig. 2, dark red time series).

3.2. Climate drivers of regional beech growth

Regional beech growth was strongly driven by moisture conditions in the current and previous growing season. Seasons with the highest correlation between radial growth and SPEI were $July_{3–12}$ of the growing season (all $r > 0.51, p < 0.001$) and $September_3$ of the previous year ($r = 0.47$, $p < 0.001$, Fig. 3a). Correlation patterns and strength with precipitation sums and soil matric potential were very similar to SPEI (Fig. S5). The correlation pattern using mean maximum temperatures was inverse to SPEI but yielded an additional significant season of influence in $January_3$ ($r = 0.27, p < 0.05$, Fig. 3b).

For the 1931–2017 period, we found a strong increase in growth sensitivity to SPEI of previous $September_4$ ($pSep_4$) with increasing stand-level damage class, which was significantly different between the low and the high damage class ($p = 0.04$, tested via interaction $SPEI_{pSep4} \times$ damage class). The most parsimonious model also included soil matric potential of current year $August_6$, $June_1$ precipitation, and $January_3$ mean maximum temperatures (Table 2). The higher climate sensitivity in stands with higher crown damage also agreed with the higher standard deviation of the spline-detrended damage-level chronologies (Table 2).

In the recent 1971–2016 period, mast index (Fig. S6) was a significant driver of year-to-year growth variability (Table 3). The selected climate variables and strength of climate sensitivities were similar compared to the longer period (i.e., 1931–2017). Here, we also found higher regression coefficients for most climate variables in stands with higher crown damage. The stand-level analysis revealed a strong negative relationship between the stand-specific year-to-year growth variability (defined as the standard deviation of the spline-detrended chronologies over the 1971–2016 period) and stand variables characterizing average soil water availability, such as soil depth, AWC, and canopy height (Fig. 4). Year-to-year growth variability at tree level was negatively related to both canopy height ($p < 0.05$) and absolute growth rate (BAI, $p < 0.001$; marginal $R^2 = 0.27$, conditional $R^2 = 0.36$, Table S1).

3.3. Generalized linear models of individual tree crown damage

The generalized linear models revealed that TCL was lower in trees with higher absolute growth rates (BAI, $p = 0.001$) and stands with deeper soils (soil depth, $p = 0.03$, Table 4). CT was also found to be lower in stands with deeper soils ($p < 0.01$) and in trees with higher DBH ($p = 0.06$), meaning larger trees had less crown damage in 2021.

3.4. Principal component analysis

The first two principal components explained together 50% of the total variance and revealed two clear data orientations (Fig. 5). Across stands, the variables were predominantly oriented from (top) left to (bottom) right, and within stands, variables were oriented from bottom left to top right. Stands with higher AWC, and taller trees were oppositely arranged from stands being more sensitive to climate, i.e., that have a generally higher year-to-year variability (sd) and show steeper regression coefficients to SPEI or soil matric potential. TCL and CT were aligned in the same direction as tree-level competition index, SD, and climate sensitivity, and opposite to DBH and absolute and size-independent growth rate (BAI and BAIstd). This ordination was further supported by the linear mixed-effects model showing that the growth rates over the 2008–2017 period were strongly influenced by competition ($p < 0.05$) and DBH ($p < 0.001$, marginal $R^2 = 0.42$; conditional $R^2 = 0.52$, Table S1).

Because growth rate was found as one of the strongest predictors of crown damage in the generalized linear mixed-effects models and was

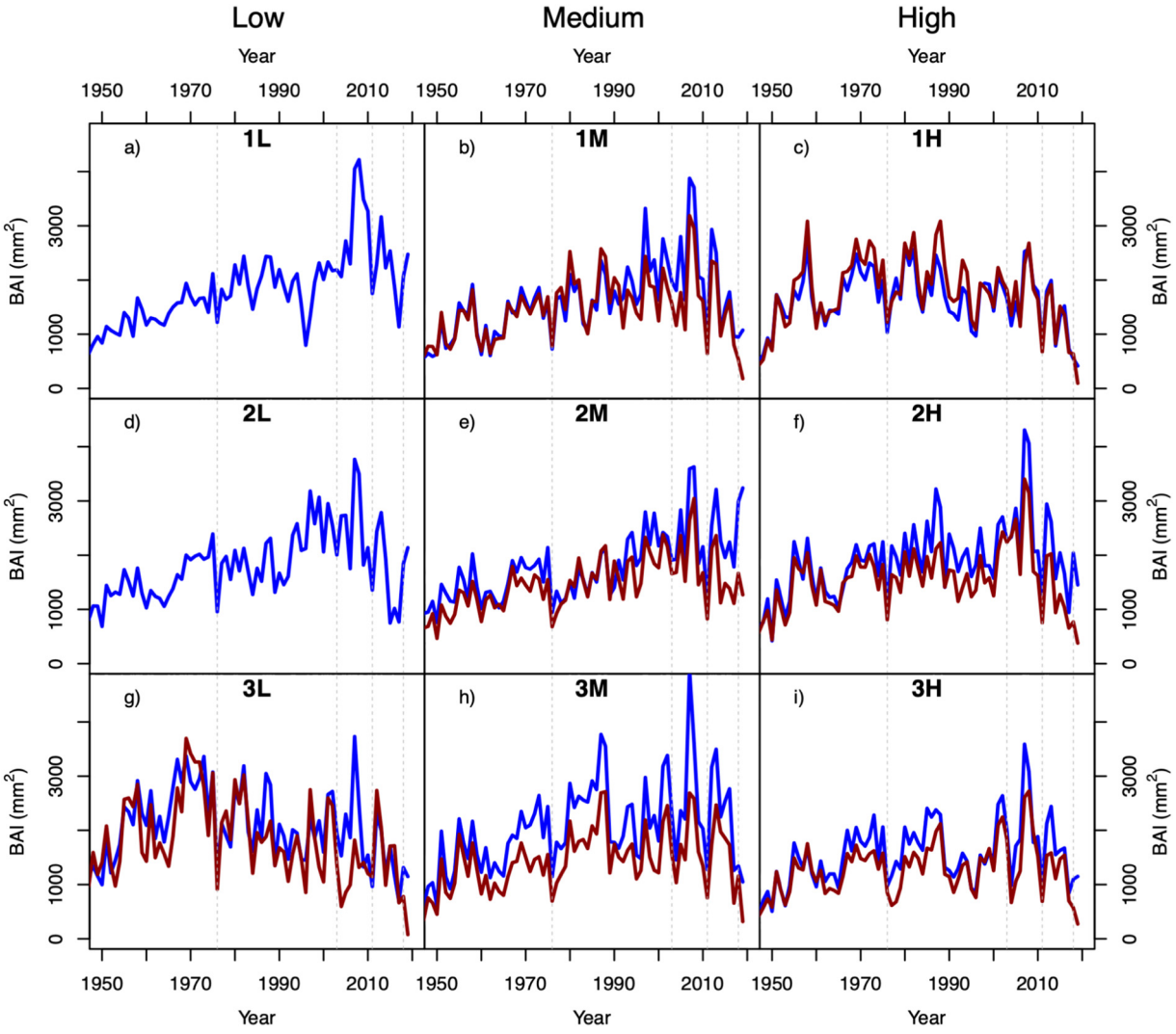

Fig. 2. Bi-weight robust mean basal area increment (BAI) time series of trees with TCL2021 (total crown biomass loss in 2021) < 50% and ≥ 50% in blue and red, respectively. Stands are ordered from left to right showing increasing stand-level crown damage from low (L), medium (M) to high (H) crown damage. There was only one (no) tree with ≥ 50% TCL in stand 1L (2L). Vertical dashed lines denote the four driest SPEI August$_6$ years since 1950: 1976, 2003, 2011, and 2018. Time series end in 2019.

additionally oriented directly opposite to crown damage in the first two principal components, we re-classified trees with TCL <50% and ≥50%. This revealed that in six out of seven stands (two stands did not have enough trees with ≥50% TCL to form a mean chronology, Table 1) trees with higher post-drought crown damage had been indeed growing slower for a long time (Fig. 2b, e, f, h, i). Even corrected for tree size, growth rates of less damaged trees were on average 7–28% higher compared to heavily damaged trees since 1971 (Fig. S7).

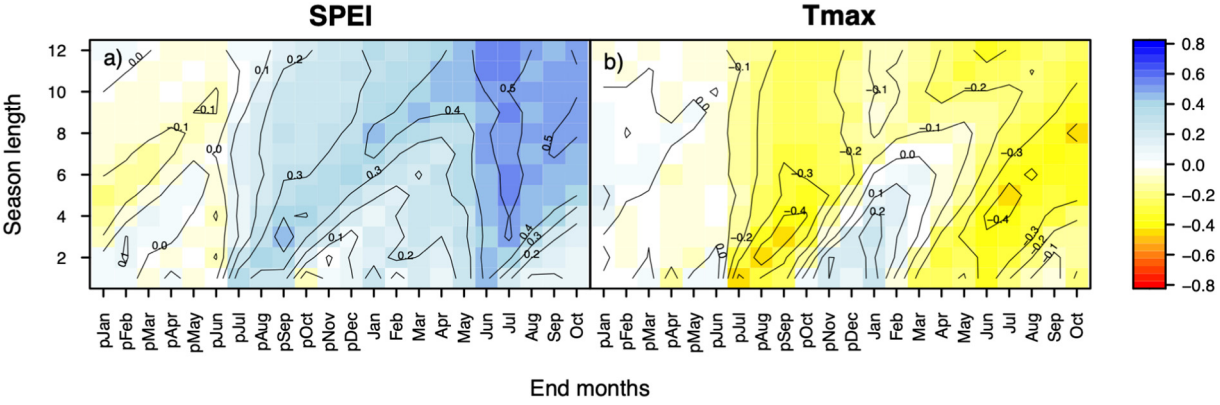

Fig. 3. Heat maps showing the Spearman rank correlations between the spline-detrended regional chronology and Standardized Precipitation-Evapotranspiration Index (SPEI) (a) and mean maximum temperature (b) from previous January to current year October. Y-axis shows correlations with a season length of one month to 12 months.

Table 2
Coefficients of the multiple regression of radial growth against climate parameters over the 1931–2017 period. All time series were detrended with a 30-year spline. SMP: soil matric potential; R^2_{adj}: adjusted R^2 of the multiple regression; SD: standard deviation of the chronologies; ACF: first-order auto-correlation coefficient of the chronologies. Coefficients in bold (bold italic) were significant at $p < 0.05$ ($p < 0.001$).

Damage class	SPEI $pSep_4$	SMP Aug_6	PPT Jun_1	Tmax Jan_3	R^2_{adj}	SD	ACF
All	***0.111***	***0.091***	**0.047**	***0.062***	0.568	0.23	0.19
Low	***0.084***	***0.086***	0.037	***0.055***	0.507	0.20	0.17
Medium	***0.122***	***0.099***	**0.052**	**0.060**	0.545	0.25	0.21
High	***0.140***	***0.099***	**0.050**	**0.069**	0.514	0.27	0.33

Table 3
Coefficients of the multiple regression of radial growth against climate parameters over the 1971–2016 period. All time series were detrended with a 30-year spline. R^2_{adj}: adjusted R^2 of the multiple regression; SD: standard deviation of the chronologies. ACF: first-order auto-correlation coefficient of the chronologies. Coefficients in bold (bold italic) were significant at $p < 0.05$ ($p < 0.001$).

Damage class	SPEI $pSep_4$	SPEI Aug_6	PPT Jun_1	Tmax Jan_3	Mast index	R^2_{adj}	SD	ACF
All	***0.112***	**0.056**	***0.116***	0.039	**−0.074**	0.551	0.23	0.06
Low	***0.099***	**0.074**	**0.096**	0.031	**−0.069**	0.558	0.22	0.11
Medium	***0.122***	0.050	***0.135***	0.037	**−0.083**	0.515	0.26	0.09
High	**0.123**	0.051	**0.118**	0.038	**−0.084**	0.419	0.27	0.19

4. Discussion

We showed that the 2018 summer drought in northwestern Switzerland led to higher crown damage on sites with lower soil water availability and in trees showing lower growth rates in the recent past. Lower overall soil water availability was proportional to year-to-year variability in radial growth, which was also evidenced by higher regression coefficients of SPEI, especially that of previous year late summer. Tree-individual analyses revealed that within-site crown damage was higher in trees with lower growth rates, higher year-to-year variability in radial growth, and higher competition indexes. All the presented analyses point towards tree vigor before the 2018 extreme drought and soil water availability as primary drivers for drought-induced crown dieback severity.

Table 4
Log-odds of the generalized linear mixed-effects models predicting crown transparency (CT) and total crown biomass loss (TCL). Marginal and conditional R^2 (R^2m and R^2c) were calculated following the delta method in R package *MuMIn*. Only model summaries within ΔBIC < 2 of the most parsimonious models are shown. Significance levels: ***$p < 0.001$; **$p < 0.01$; *$p < 0.05$; '$p < 0.1$.

	Intercept	BAI	Soil depth	DBH	ΔBIC	R^2m	R^2c
TCL	−0.75**	−0.75**				0.10	0.18
	−0.77**	−0.69**	−0.51*		1.3	0.16	0.20
CT	−1.83***		−0.95***			0.12	0.12
	−1.87***		−0.74**	−0.47'	1.1	0.13	0.13

4.1. Higher climate sensitivity of radial growth at sites with lower soil water availability

Our findings that trees are more sensitive to variability in climatic water balance (SPEI) at sites with lower soil water availability are consistent with the literature: It has long been demonstrated that the closer to the edge of a tree species' distribution, or at sites with marginal growing conditions (e.g., sites with lower soil water availability, Rabbel et al., 2018), the greater the sensitivity of radial growth to climate (Fritts et al., 1965; Klesse et al., 2020; Rigling et al., 2002). Even though climatic conditions are very similar across our sites (range: 0.5 °C mean annual temperature, 50 mm mean annual precipitation), soil properties clearly modulate growth sensitivity to meteorological moisture variability, leading to a 1.6-fold stronger impact of previous summer SPEI ($pSep_4$) between the least and most damaged sites (Table 2). These observations follow Liebig's law of the minimum (Liebig, 1841) that postulates the more limiting a variable is to a process, the more sensitive this process becomes to variations of that variable. The increasing importance of a single growth-limiting factor is also reflected in increased growth synchrony at sites with lower soil moisture availability (see rbar in Table 1, Tejedor et al., 2020). Altogether, our results highlight the need for ecologically unbiased and finely resolved tree-ring networks to representatively assess climate change impacts on forest growth across large scales (Evans et al., 2021; Klesse et al., 2018b).

The 2018 drought did not particularly lead to narrow rings in 2018 in the 189 studied beech trees (Figs. 3, S4), and neither did it at many other sites across Central Europe as evidenced through dendrometer measurements (Salomón et al., 2022). This is not totally surprising, because on average, only 23% of annual radial increment in lowland beech in Switzerland is produced after July 1st, i.e., the time when drought conditions worsened considerably in 2018 (Etzold et al., 2022; Zweifel et al., 2020). However,

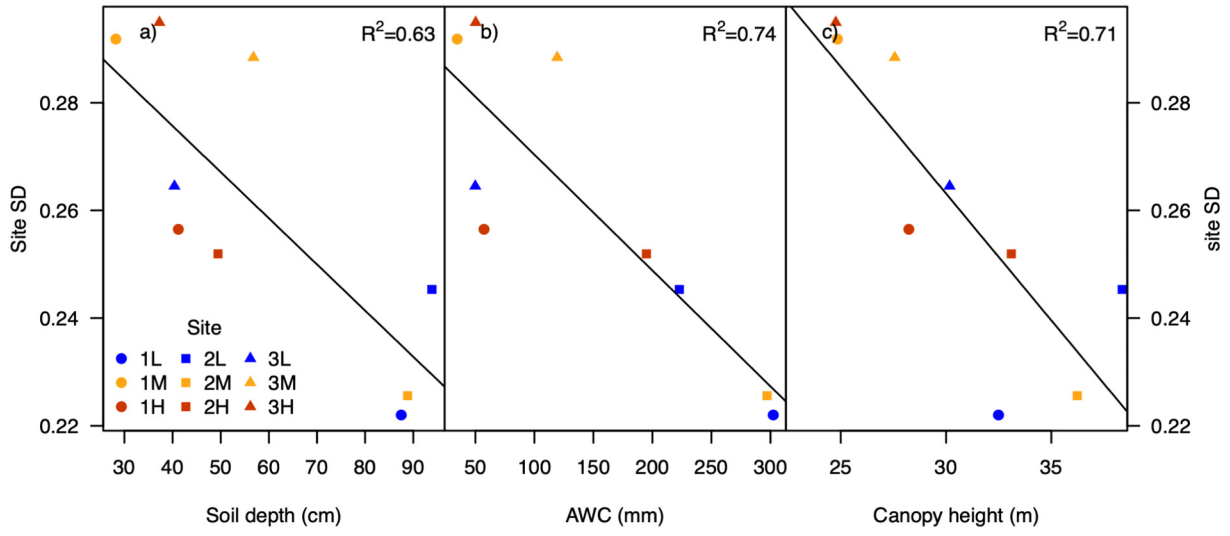

Fig. 4. Linear regressions of the standard deviation (SD) of spline-detrended stand chronologies over the 1971–2016 period against a) soil depth, b) plant-available soil water storage capacity (AWC), and c) canopy height. L, M, and H, mean low, medium, and high stand-level crown damage, respectively.

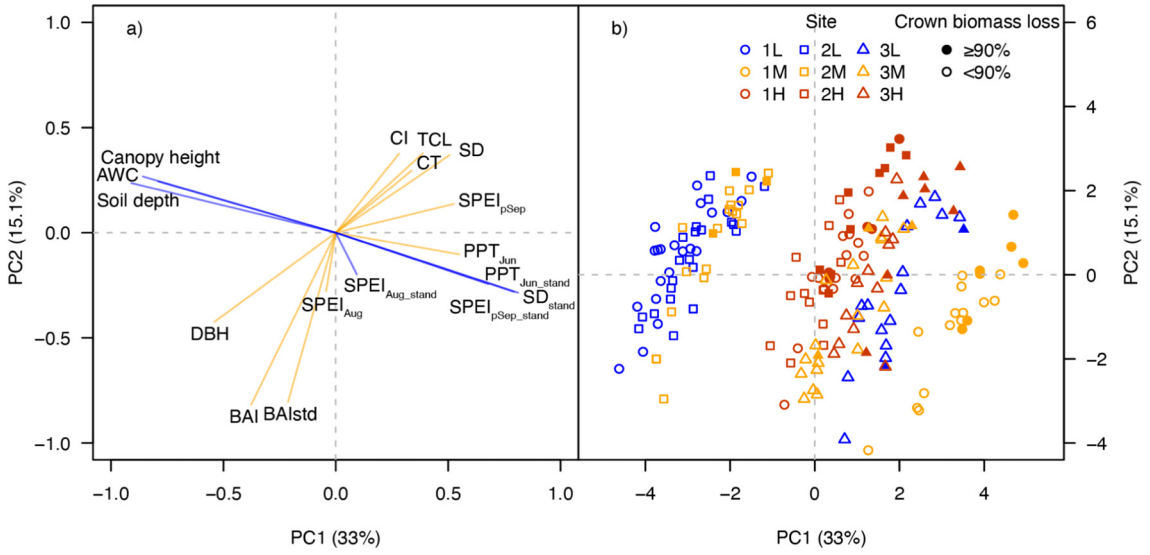

Fig. 5. (a) Loadings of the explanatory stand- (blue) and tree-level (orange) variables on the first two principal components and (b) tree individual values multiplied with the first two eigenvectors of the principal component analysis. Filled (open) circles denote the trees with ≥ 90% (< 90%) TCL in 2021. AWC: Available water capacity, CI: competition index, DBH: diameter at breast height, BAI: basal area increment (2008–2017), BAIstd: size-detrended BAI (2008–2017), TCL: total crown biomass loss, CT: crown transparency, SD: standard deviation of the spline-detrended growth time series (1971–2016). SPEI and PPT: regression coefficients to SPEI and precipitation (1971–2016). If there are multiple levels for a variable, subscript _stand denotes stand-level variables, no subscript denotes tree-level variables.

we showed that late summer droughts have a strong influence on radial tree growth in the following year (Fig. 3), in agreement with the delayed growth response reported by Hacket-Pain et al. (2016) and Mausolf et al. (2018). The increased frequency of drought extremes during the last 20 years (Fig. S1) and negative growth trends in most stands (Fig. 2) might thus have aggravated the impact of the 2018 drought on tree health.

4.2. Higher crown damage at sites with lower soil water storage capacity and higher climate sensitivity

Our results support the often observed pattern that higher growth variability or directly inferred drought sensitivity of radial growth indicates a higher vulnerability to drought-induced crown damage and mortality (Cailleret et al., 2019; Keen et al., 2022; Linares and Camarero, 2012; Tables 2 and 3, Fig. 5). Given the similar age of the nine stands, we showed that canopy heights reflect site productivity, which, under similar climate conditions, is predominantly driven by average soil water availability (Fig. 2). Deeper soils (as evidenced by soil profiles and taller canopy heights) in less damaged stands provided trees with a buffer to overcome the prolonged soil water deficit that developed during the 2018 summer and prevented premature leaf senescence (Chakraborty et al., 2017; Leuschner, 2020; Lévesque et al., 2016; Walthert et al., 2021). This agrees with Brun et al. (2020) who showed that early leaf wilting in Switzerland in 2018 was less pronounced with increasing vegetation height, i.e., in stands with less hydraulic limitation. Here, greater tree height seems not to be an intrinsic predisposing factor for sensitivity to hydraulic failure (as shown by Grote et al., 2016, McDowell and Allen, 2015, or Stovall et al., 2019) but rather an indicator for generally higher water availability that also sustains the water demand in dry years.

If early leaf senescence as strategy to avoid the formation of embolisms in branches had been successful, i.e. preventing hydraulic failure and desiccation (Bréda et al., 2006; Marchin et al., 2010; Schuldt et al., 2020), we would not have expected such strong and long-lasting effects on crown dieback in the following years. We thus interpret the premature leaf senescence during the severe 2018 drought and the subsequent crown dieback as a consequence of irreversible hydraulic failure in the branches caused by extremely low soil water potentials (Arend et al., 2022, 2021; Choat et al., 2018; Walthert et al., 2021; Wohlgemuth et al., 2020).

4.3. Higher crown damage in smaller, slower-growing trees

We showed that growth variability was lower in stands with taller and less damaged trees and lower in trees that grew faster (even after controlling for DBH) and that competitive pressure was a decisive driver of absolute growth rates (BAI, Table S1). Altogether, our findings point towards a soil water potential-driven growth limitation and crown damage predominantly affecting the weakest, slowest-growing trees (Fig. 5, Hülsmann et al., 2018). The reasoning is that average radial growth is primarily defined by leaf area, hence crown size. Crown size is related to DBH and tree height but is also controlled by competition for light (neighbor shading) and belowground resource availability (size of root system, soil nutrients, and water availability). Two trees in the same stand with the same DBH should in principle grow similarly. Yet, if one tree consistently grows less, it is likely that this tree had overall fewer resources, either through an already smaller crown because of shading through neighboring trees, through increased competition for belowground resources, or due to less favorable micro-site conditions (e.g., shallow soils with limited water availability) leading to less root biomass and reduced photosynthetic capacity. Water limitation, particularly less access to deep soil water pools – derived through lower tree heights and $\delta^{18}O$ enriched xylem water – was previously found as a determining factor for drought-induced mortality in oaks in Italy (Colangelo et al., 2017; Ripullone et al., 2020). Lower growth rates for a prolonged period preceding tree mortality is a well-documented phenomenon (Cailleret et al., 2016). There are, however, contrasting results showing that trees, which were growing faster in the past, were also more prone to drought-induced mortality in extremely dry years (e.g., Gessler et al., 2018; Voltas et al., 2013). These authors assumed that trees that grow normally under non-restricted water supply and otherwise favorable growing conditions develop architectures with large crowns, high shoot-to-root ratios, and cavity-prone wide xylem vessels making them susceptible to hydraulic failure. In our study, however, potentially better access to soil water resources may have compensated for such potentially negative acclimation or frequent water limitation might have avoided long-term overbuilding of the canopy also in faster-growing trees. Taken together, if climate conditions in a particular year are much less favorable than average it is likely that trees historically growing in worse micro-site conditions and with less access to deeper soil water pools (which is likely

reflected in higher interannual growth variability), and/or in a more competitive environment (lower average growth rate), would be more impacted by extreme climatic events.

Previous studies have shown that beech tree's tolerance to extreme environmental conditions is to some extent under genetic control (Cuervo-Alarcon et al., 2021; Isaac-Renton et al., 2018; Stojnić et al., 2018), which is also known to influence growth rates of different genotypes (Leuschner, 2020). Still, the degree to which genetic variability within and across our investigated stands contributes to the observed responses is unknown and further studies are needed.

4.4. Implications for the future of beech in central Europe

Our findings imply that less dense stands could buffer the effect of future extreme droughts predicted to occur more frequently. While there is both conflicting and site and species-specific evidence on how thinning influences the sensitivity of tree growth to droughts (Bosela et al., 2021; Diaconu et al., 2017; Mausolf et al., 2018; Sohn et al., 2016), it certainly temporarily alleviates competition for water and thus should reduce peak drought stress experienced by trees, especially in sites with low soil water storage capacity (Giuggiola et al., 2018, 2016). The 2018 drought was among the most severe droughts of the last 150 years (Erfurt et al., 2020; Rathgeb et al., 2020). Yet, most mesic beech stands at low elevation in Central Europe were largely unaffected by this drought. We conclude that in such stands with possibly deep soils and good water holding capacity, beech is likely not immediately threatened by current and future droughts, even though future growth is projected to decrease throughout the species' range (Martinez del Castillo et al., 2022). However, it is likely that forest health conditions between optimal sites and sites with marginal growth conditions will diverge further under continued exposure to extreme water deficit, which is amplified by phenological shifts leading to an earlier start of the growing season and thus a prolonged water loss through transpiration (Meier et al., 2021).

5. Conclusions

Our study contributes to the rapidly growing body of literature investigating the effects of tree size, competition, and growth rate on drought-induced dieback. We investigated beech growth and crown damage across various site conditions and showed that crown damage was the highest on the driest sites with shallower soils and in smaller and slower-growing trees.

Overall, our findings suggest a decrease in the competitive ability of beech and in its abundance on suboptimal sites in the lowlands and a retreat to sites with better water retention capacity. However, complete disappearance of beech is not to be expected.

CRediT authorship contribution statement

S. Klesse – Methodology, Formal Analysis, Visualization, Writing original draft.

Wohlgemuth T. – Conceptualization, Methodology, Project administration, Writing original draft.

Meusburger K., Investigation, Writing – original draft, Methodology.

Vitasse Y., Conceptualization, Methodology, Writing original draft.

von Arx G., Conceptualization, Writing original draft, Methodology.

Lévesque M., Writing – original draft, Methodology.

Neycken A., Writing – original draft, Methodology.

Braun S., Writing - Review & Editing.

Dubach V., Writing - Review & Editing.

Gessler A., Writing - Review & Editing.

Ginzler C., Writing - Review & Editing, Investigation,

Gossner M.M., Writing - Review & Editing.

Hagedorn F., Writing - Review & Editing.

Queloz V., Writing - Review & Editing.

Samblàs Vives E. – Investigation, Writing - Review & Editing.

Rigling A., Conceptualization, Writing - Review & Editing.

Frei E.R. – Conceptualization, Methodology, Data curation, Project administration, Writing original draft.

Data availability

Data will be made available on request.

Declaration of competing interest

None declared.

Acknowledgments

We thank Roger Köchli, Leo Loprieno, Maurice Moor, Daniel Pock, Silas Strebel, Ide Uitentuis, Ueli Wasem, and other people for preparing and conducting the fieldwork, as well as Daniel Nievergelt, Martin Kistler and Raphael Sigrist for training the field crews. We further thank Anne Verstege and Daniel Pock for their help with the preparation of the cores and ring width measurements. We acknowledge Daniel Scherrer and Dirk Schmatz for providing the interpolated climate data. Furthermore, we thank the cantonal authorities of the canton of Jura, the regional forest authorities, and private forest owners for providing us the permission and access to conduct this monitoring project.

SK was supported by the SwissForestLab (Research Grant SFL20 P5), and by the Federal Office for the Environment FOEN. We are grateful to the WSL drought initiative and the WHFF-CH fund (Project 2019.15) for financial support.

Appendix A. Supplementary data

Supplementary data to this article can be found online at https://doi.org/10.1016/j.scitotenv.2022.157926.

References

Allen, C.D., Macalady, A.K., Chenchouni, H., Bachelet, D., McDowell, N., Vennetier, M., Kitzberger, T., Rigling, A., Breshears, D.D., Hogg, E.H.(Ted), Gonzalez, P., Fensham, R., Zhang, Z., Castro, J., Demidova, N., Lim, J.-H., Allard, G., Running, S.W., Semerci, A., Cobb, N., 2010. A global overview of drought and heat-induced tree mortality reveals emerging climate change risks for forests. For. Ecol. Manag. 259, 660–684. https://doi.org/10.1016/j.foreco.2009.09.001.

Allen, C.D., Breshears, D.D., McDowell, N.G., 2015. On underestimation of global vulnerability to tree mortality and forest die-off from hotter drought in the Anthropocene. Ecosphere 6, 1–55. https://doi.org/10.1890/ES15-00203.1.

Anderegg, W.R.L., Kane, J.M., Anderegg, L.D.L., 2013. Consequences of widespread tree mortality triggered by drought and temperature stress. Nat. Clim. Chang. 3, 30–36. https://doi.org/10.1038/nclimate1635.

Anderegg, W.R.L., Trugman, A.T., Badgley, G., Anderson, C.M., Bartuska, A., Ciais, P., Cullenward, D., Field, C.B., Freeman, J., Goetz, S.J., Hicke, J.A., Huntzinger, D., Jackson, R.B., Nickerson, J., Pacala, S., Randerson, J.T., 2020. Climate-driven risks to the climate mitigation potential of forests. Science 368, eaaz7005. https://doi.org/10.1126/science.aaz7005.

Arend, M., Link, R.M., Patthey, R., Hoch, G., Schuldt, B., Kahmen, A., 2021. Rapid hydraulic collapse as cause of drought-induced mortality in conifers. Proc. Natl. Acad. Sci. 118. https://doi.org/10.1073/pnas.2025251118.

Arend, M., Link, R.M., Zahnd, C., Hoch, G., Schuldt, B., Kahmen, A., 2022. Lack of hydraulic recovery as a cause of post-drought foliage reduction and canopy decline in European beech. New Phytol. 234, 1195–1205. https://doi.org/10.1111/nph.18065.

Ascoli, D., Maringer, J., Hacket-Pain, A., Conedera, M., Drobyshev, I., Motta, R., Cirolli, M., Kantorowicz, W., Zang, C., Schueler, S., Croisé, L., Piussi, P., Berretti, R., Palaghianu, C., Westergren, M., Lageard, J.G.A., Burkart, A., Bichsel, R.G., Thomas, P.A., Beudert, B., Övergaard, R., Vacchiano, G., 2017. Two centuries of masting data for European beech and Norway spruce across the European continent. 5th ed. Ecology 98, 1473. https://doi.org/10.1002/ecy.1785.

Baltensweiler, A., Brun, P., Pranga, J., Psomas, A., Zimmermann, N.E., Ginzler, C., 2020. Räumliche Analyse von Trockenheitssymptomen im Schweizer Wald mit Sentinel-2-Satellitendaten. Schweiz. Z. Forstwes. 298–301. https://doi.org/10.3188/szf.2020.0298.

Bartoń, K., 2018. MuMIn: Multi-Model Inference. R package version 1.42.1.

Bastin, J.-F., Finegold, Y., Garcia, C., Mollicone, D., Rezende, M., Routh, D., Zohner, C.M., Crowther, T.W., 2019. The global tree restoration potential. Science 365, 76–79. https://doi.org/10.1126/science.aax0848.

Bates, D., Mächler, M., Bolker, B., Walker, S., 2015. Fitting linear mixed-effects models using lme4. J. Stat. Softw. 67, 1–48. https://doi.org/10.18637/jss.v067.i01.

Beguería, S., Vicente-Serrano, S.M., 2017. SPEI: Calculation of the Standardised Precipitation-Evapotranspiration Index. R Package version 1.7.

Bennett, A.C., McDowell, N.G., Allen, C.D., Anderson-Teixeira, K.J., 2015. Larger trees suffer most during drought in forests worldwide. Nat. Plants 1, 1–5. https://doi.org/10.1038/nplants.2015.139.

Bigler, C., Vitasse, Y., 2021. Premature leaf discoloration of European deciduous trees is caused by drought and heat in late spring and cold spells in early fall. Agric. For. Meteorol. 307, 108492. https://doi.org/10.1016/j.agrformet.2021.108492.

Bosela, M., Štefančík, I., Marčiš, P., Rubio-Cuadrado, Á., Lukac, M., 2021. Thinning decreases above-ground biomass increment in central European beech forests but does not change individual tree resistance to climate events. Agric. For. Meteorol. 306, 108441. https://doi.org/10.1016/j.agrformet.2021.108441.

Braun, S., Schindler, C., Rihm, B., 2017. Growth trends of beech and Norway spruce in Switzerland: the role of nitrogen deposition, ozone, mineral nutrition and climate. Sci. Total Environ. 599–600, 637–646. https://doi.org/10.1016/j.scitotenv.2017.04.230.

Bréda, N., Huc, R., Granier, A., Dreyer, E., 2006. Temperate forest trees and stands under severe drought: a review of ecophysiological responses, adaptation processes and long-term consequences. Ann. For. Sci. 63, 625–644. https://doi.org/10.1051/forest:2006042.

Briffa, K.R., Melvin, T.M., 2011. A closer look at regional curve standardization of tree-ring records: justification of the need, a warning of some pitfalls, and suggested improvements in its application. Dendroclimatology. Springer, pp. 113–145.

Brun, P., Psomas, A., Ginzler, C., Thuiller, W., Zappa, M., Zimmermann, N.E., 2020. Large-scale early-wilting response of central European forests to the 2018 extreme drought. Glob. Change Biol. 26, 7021–7035. https://doi.org/10.1111/gcb.15360.

Buchman, R.G., Pederson, S.P., Walters, N.R., 1983. A tree survival model with application to species of the Great Lakes region. Can. J. For. Res. 13, 601–608. https://doi.org/10.1139/x83-087.

Bunn, A., Korpela, M., Biondi, F., Campelo, F., Mérian, P., Qeadan, F., Zang, C., 2019. dplR: Dendrochronology Program Library in R. R package version 1.7.0.

Cailleret, M., Jansen, S., Robert, E.M.R., Desoto, L., Aakala, T., Antos, J.A., Beikircher, B., Bigler, C., Bugmann, H., Caccianiga, M., Čada, V., Camarero, J.J., Cherubini, P., Cochard, H., Coyea, M.R., Čufar, K., Das, A.J., Davi, H., Delzon, S., Dorman, M., Gea-Izquierdo, G., Gillner, S., Haavik, L.J., Hartmann, H., Hereş, A.-M., Hultine, K.R., Janda, P., Kane, J.M., Kharuk, V.I., Kitzberger, T., Klein, T., Kramer, K., Lens, F., Levanic, T., Linares Calderon, J.C., Lloret, F., Lobo-Do-Vale, R., Lombardi, F., López Rodríguez, R., Mäkinen, H., Mayr, S., Mészáros, I., Metsaranta, J.M., Minunno, F., Oberhuber, W., Papadopoulos, A., Peltoniemi, M., Petritan, A.M., Rohner, B., Sangüesa-Barreda, G., Sarris, D., Smith, J.M., Stan, A.B., Sterck, F., Stojanović, D.B., Suarez, M.L., Svoboda, M., Tognetti, R., Torres-Ruiz, J.M., Trotsiuk, V., Villalba, R., Vodde, F., Westwood, A.R., Wyckoff, P.H., Zafirov, N., Martínez-Vilalta, J., 2016. A synthesis of radial growth patterns preceding tree mortality. Glob. Change Biol. https://doi.org/10.1111/gcb.13535.

Cailleret, M., Dakos, V., Jansen, S., Robert, E.M.R., Aakala, T., Amoroso, M.M., Antos, J.A., Bigler, C., Bugmann, H., Caccianaga, M., Camarero, J.-J., Cherubini, P., Coyea, M.R., Čufar, K., Das, A.J., Davi, H., Gea-Izquierdo, G., Gillner, S., Haavik, L.J., Hartmann, H., Hereş, A.-M., Hultine, K.R., Janda, P., Kane, J.M., Kharuk, V.I., Kitzberger, T., Klein, T., Levanic, T., Linares, J.-C., Lombardi, F., Mäkinen, H., Mészáros, I., Metsaranta, J.M., Oberhuber, W., Papadopoulos, A., Petritan, A.M., Rohner, B., Sangüesa-Barreda, G., Smith, J.M., Stan, A.B., Stojanovic, D.B., Suarez, M.-L., Svoboda, M., Trotsiuk, V., Villalba, R., Westwood, A.R., Wyckoff, P.H., Martínez-Vilalta, J., 2019. Early-warning signals of individual tree mortality based on annual radial growth. Front. Plant Sci. 9. https://doi.org/10.3389/fpls.2018.01964.

Chakraborty, T., Saha, S., Matzarakis, A., Reif, A., 2017. Influence of multiple biotic and abiotic factors on the crown die-back of European beech trees at their drought limit. Flora 229, 58–70. https://doi.org/10.1016/j.flora.2017.02.012.

Choat, B., Brodribb, T.J., Brodersen, C.R., Duursma, R.A., López, R., Medlyn, B.E., 2018. Triggers of tree mortality under drought. Nature 558, 531–539. https://doi.org/10.1038/s41586-018-0240-x.

Ciais, P., Reichstein, M., Viovy, N., Granier, A., Ogée, J., Allard, V., Aubinet, M., Buchmann, N., Bernhofer, C., Carrara, A., Chevallier, F., De Noblet, N., Friend, A.D., Friedlingstein, P., Grünwald, T., Heinesch, B., Keronen, P., Knohl, A., Krinner, G., Loustau, D., Manca, G., Matteucci, G., Miglietta, F., Ourcival, J.M., Papale, D., Pilegaard, K., Rambal, S., Seufert, G., Soussana, J.F., Sanz, M.J., Schulze, E.D., Vesala, T., Valentini, R., 2005. Europe-wide reduction in primary productivity caused by the heat and drought in 2003. Nature 437, 529–533. https://doi.org/10.1038/nature03972.

Colangelo, M., Camarero, J.J., Borghetti, M., Gazol, A., Gentilesca, T., Ripullone, F., 2017. Size matters a lot: drought-affected Italian oaks are smaller and show lower growth prior to tree death. Front. Plant Sci. 8. https://doi.org/10.3389/fpls.2017.00135.

Cook, B.I., Smerdon, J.E., Seager, R., Coats, S., 2014. Global warming and 21st century drying. Clim. Dyn. 43, 2607–2627. https://doi.org/10.1007/s00382-014-2075-y.

Copernicus Open Access Hub, 2022 [WWW Document] URL (accessed 6.20.22).

Cuervo-Alarcon, L., Arend, M., Müller, M., Sperisen, C., Finkeldey, R., Krutovsky, K.V., 2021. A candidate gene association analysis identifies SNPs potentially involved in drought tolerance in European beech (*Fagus sylvatica* L.). Sci. Rep. 11, 2386. https://doi.org/10.1038/s41598-021-81594-w.

Diaconu, D., Kahle, H.-P., Spiecker, H., 2017. Thinning increases drought tolerance of European beech: a case study on two forested slopes on opposite sides of a valley. Eur. J. For. Res. 136, 319–328. https://doi.org/10.1007/s10342-017-1033-8.

Dobbertin, M., Hug, C., Schwyzer, A., Borer, S., Schmalz, H., 2016. Kronenansprachen auf den Sanasilva- und den LWF-Flächen. Swiss Fed. Res. Inst. WSL, Birmensdorf. https://www.wsl.ch/fileadmin/user_upload/WSL/Wald/Waldentwicklung_Monitoring/LWF/Sanasilva/ssi_anleitung_v10_extern.pdf.

Eichhorn, J., Roskams, P., Potocic, N., Timmermann, V., Ferretti, M., Mues, V., Szepesi, A., Durrant, D., Seletkovic, I., Schroeck, H.-W., Nevalainen, S., Bussotti, F., Garcia, P., Wulff, S., 2020. Part IV: visual assessment of crown condition and damaging agents. Manual on Methods and Criteria for Harmonized Sampling, Assessment, Monitoring and Analysis of the Effects of Air Pollution on Forests. Thünen Institute of Forest Ecosystems, Eberswalde, Germany.

Erfurt, M., Skiadaresis, G., Tijdeman, E., Blauhut, V., Bauhus, J., Glaser, R., Schwarz, J., Tegel, W., Stahl, K., 2020. A multidisciplinary drought catalogue for southwestern Germany dating back to 1801. Nat. Hazards Earth Syst. Sci. 20, 2979–2995. https://doi.org/10.5194/nhess-20-2979-2020.

Etzold, S., Sterck, F., Bose, A.K., Braun, S., Buchmann, N., Eugster, W., Gessler, A., Kahmen, A., Peters, R.L., Vitasse, Y., Walthert, L., Ziemińska, K., Zweifel, R., 2022. Number of growth days and not length of the growth period determines radial stem growth of temperate trees. Ecol. Lett. 25, 427–439. https://doi.org/10.1111/ele.13933.

Evans, M.E.K., DeRose, R.J., Klesse, S., Girardin, M.P., Heilman, K.A., Alexander, M.R., Arsenault, A., Babst, F., Bouchard, M., Cahoon, S.M.P., Campbell, E.M., Dietze, M., Duchesne, L., Frank, D.C., Giebink, C.L., Gómez-Guerrero, A., García, G.G., Hogg, E.H., Metsaranta, J., Ols, C., Rayback, S.A., Reid, A., Ricker, M., Schaberg, P.G., Shaw, J.D., Sullivan, P.F., GaytÁn, S.A.V., 2021. Adding tree rings to North America's National Forest Inventories: an essential tool to guide drawdown of atmospheric CO_2. BioScience 72 (3), 233–246. https://doi.org/10.1093/biosci/biab119.

Frei, E.R., Gossner, M.M., Vitasse, Y., Queloz, V., Dubach, V., Gessler, A., Ginzler, C., Hagedorn, F., Meusburger, K., Moor, M., Samblás Vives, E., Rigling, A., Uitentuis, I., von Arx, G., Wohlgemuth, T., 2022. European beech dieback after premature leaf senescence during the 2018 drought in northern Switzerland. Plant Biol. Submitted for publication.

Fritts, H.C., Smith, D.G., Cardis, J.W., Budelsky, C.A., 1965. Tree-ring characteristics along a vegetation gradient in northern Arizona. Ecology 46, 393–401. https://doi.org/10.2307/1934872.

Gao, B., 1996. NDWI—a normalized difference water index for remote sensing of vegetation liquid water from space. Remote Sens. Environ. 58, 257–266. https://doi.org/10.1016/S0034-4257(96)00067-3.

Gärtner, H., Nievergelt, D., 2010. The core-microtome: a new tool for surface preparation on cores and time series analysis of varying cell parameters. Dendrochronologia 28, 85–92. https://doi.org/10.1016/j.dendro.2009.09.002.

Gessler, A., Cailleret, M., Joseph, J., Schönbeck, L., Schaub, M., Lehmann, M., Treydte, K., Rigling, A., Timofeeva, G., Saurer, M., 2018. Drought induced tree mortality – a tree-ring isotope based conceptual model to assess mechanisms and predispositions. New Phytol. 219, 485–490. https://doi.org/10.1111/nph.15154.

Gillner, S., Rüger, N., Roloff, A., Berger, U., 2013. Low relative growth rates predict future mortality of common beech (*Fagus sylvatica* L.). For. Ecol. Manag. 302, 372–378. https://doi.org/10.1016/j.foreco.2013.03.032.

Giuggiola, A., Ogée, J., Rigling, A., Gessler, A., Bugmann, H., Treydte, K., 2016. Improvement of water and light availability after thinning at a xeric site: which matters more? A dual isotope approach. New Phytol. 210, 108–121. https://doi.org/10.1111/nph.13748.

Giuggiola, A., Zweifel, R., Feichtinger, L.M., Vollenweider, P., Bugmann, H., Haeni, M., Rigling, A., 2018. Competition for water in a xeric forest ecosystem – effects of understory removal on soil micro-climate, growth and physiology of dominant scots pine trees. For. Ecol. Manag. 409, 241–249. https://doi.org/10.1016/j.foreco.2017.11.002.

Grote, R., Gessler, A., Hommel, R., Poschenrieder, W., Priesack, E., 2016. Importance of tree height and social position for drought-related stress on tree growth and mortality. Trees 30, 1467–1482. https://doi.org/10.1007/s00468-016-1446-x.

Hacket-Pain, A.J., Cavin, L., Friend, A.D., Jump, A.S., 2016. Consistent limitation of growth by high temperature and low precipitation from range core to southern edge of European beech indicates widespread vulnerability to changing climate. Eur. J. For. Res. 135, 897–909. https://doi.org/10.1007/s10342-016-0982-7.

Hacket-Pain, A.J., Ascoli, D., Vacchiano, G., Biondi, F., Cavin, L., Conedera, M., Drobyshev, I., Liñán, I.D., Friend, A.D., Grabner, M., Hartl, C., Kreyling, J., Lebourgeois, F., Levanič, T., Menzel, A., van der Maaten, E., van der Maaten-Theunissen, M., Muffler, L., Motta, R., Roibu, C.-C., Popa, I., Scharnweber, T., Weigel, R., Wilmking, M., Zang, C.S., 2018. Climatically controlled reproduction drives interannual growth variability in a temperate tree species. Ecol. Lett. 21, 1833–1844. https://doi.org/10.1111/ele.13158.

Hammel, K., Kennel, M., Bayerische Landesanstalt für Wald und Forstwirtschaft, 2001. Charakterisierung und Analyse der Wasserverfügbarkeit und des Wasserhaushalts von Waldstandorten in Bayern mit dem Simulationsmodell BROOK90. Frank, München.

Hegyi, F., 1974. A simulation model for managing Jack pine stands. In: Fries, J. (Ed.), Growth Models for Tree and Stand Simulation, Royal College of Forestry, Department of Forest Yield Research, Research Notes. Stockholm, Sweden.

Hülsmann, L., Bugmann, H., Cailleret, M., Brang, P., 2018. How to kill a tree: empirical mortality models for 18 species and their performance in a dynamic forest model. Ecol. Appl. 28, 522–540. https://doi.org/10.1002/eap.1668.

IPCC, 2021. Climate Change 2021: The Physical Science Basis. Contribution of Working Group I to the Sixth Assessment Report of the Intergovernmental Panel on Climate Change. Cambridge University Press.

Isaac-Renton, M., Montwé, D., Hamann, A., Spiecker, H., Cherubini, P., Treydte, K., 2018. Northern forest tree populations are physiologically maladapted to drought. Nat. Commun. 9, 5254. https://doi.org/10.1038/s41467-018-07701-0.

Jump, A.S., Ruiz-Benito, P., Greenwood, S., Allen, C.D., Kitzberger, T., Fensham, R., Martínez-Vilalta, J., Lloret, F., 2017. Structural overshoot of tree growth with climate variability and the global spectrum of drought-induced forest dieback. Glob. Chang. Biol. 23, 3742–3757. https://doi.org/10.1111/gcb.13636.

Keen, R.M., Voelker, S.L., Wang, S.-Y.S., Bentz, B.J., Goulden, M.L., Dangerfield, C.R., Reed, C.C., Hood, S.M., Csank, A.Z., Dawson, T.E., Merschel, A.G., Still, C.J., 2022. Changes in tree drought sensitivity provided early warning signals to the California drought and forest mortality event. Glob. Chang. Biol. 28, 1119–1132. https://doi.org/10.1111/gcb.15973.

Klesse, S., Babst, F., Lienert, S., Spahni, R., Joos, F., Bouriaud, O., Carrer, M., Filippo, A.D., Poulter, B., Trotsiuk, V., Wilson, R., Frank, D.C., 2018a. A combined tree ring and vegetation model assessment of European Forest growth sensitivity to interannual climate variability. Glob. Biogeochem. Cycl. 32, 1226–1240. https://doi.org/10.1029/2017GB005856.

Klesse, S., DeRose, R.J., Guiterman, C.H., Lynch, A.M., O'Connor, C.D., Shaw, J.D., Evans, M.E.K., 2018b. Sampling bias overestimates climate change impacts on forest growth in the southwestern United States. Nat. Commun. 9, 5336. https://doi.org/10.1038/s41467-018-07800-y.

Klesse, S., DeRose, R.J., Babst, F., Black, B.A., Anderegg, L.D.L., Axelson, J., Ettinger, A., Griesbauer, H., Guiterman, C.H., Harley, G., Harvey, J.E., Lo, Y.-H., Lynch, A.M., O'Connor, C., Restaino, C., Sauchyn, D., Shaw, J.D., Smith, D.J., Wood, L., Villanueva-Díaz, J., Evans, M.E.K., 2020. Continental-scale tree-ring-based projection of Douglas-fir growth: testing the limits of space-for-time substitution. Glob. Chang. Biol. 26, 5146–5163. https://doi.org/10.1111/gcb.15170.

Knapp, E.E., Bernal, A.A., Kane, J.M., Fettig, C.J., North, M.P., 2021. Variable thinning and prescribed fire influence tree mortality and growth during and after a severe drought. For. Ecol. Manag. 479, 118595. https://doi.org/10.1016/j.foreco.2020.118595.

Leuschner, C., 2020. Drought response of European beech (*Fagus sylvatica* L.) – a review. Perspect. Plant Ecol. Evol. Syst. 125576. https://doi.org/10.1016/j.ppees.2020.125576.

Lévesque, M., Walthert, L., Weber, P., 2016. Soil nutrients influence growth response of temperate tree species to drought. J. Ecol. 104, 377–387. https://doi.org/10.1111/1365-2745.12519.

Liebig, J.F. von, 1841. Organic Chemistry in Its Applications to Agriculture and Physiology. J. Owen, Cambridge.

Linares, J.C., Camarero, J.J., 2012. Growth patterns and sensitivity to climate predict silver fir decline in the Spanish Pyrenees. Eur. J. For. Res. 131, 1001–1012. https://doi.org/10.1007/s10342-011-0572-7.

Marchin, R., Zeng, H., Hoffmann, W., 2010. Drought-deciduous behavior reduces nutrient losses from temperate deciduous trees under severe drought. Oecologia 163, 845–854. https://doi.org/10.1007/s00442-010-1614-4.

Martinez del Castillo, E., Zang, C.S., Buras, A., Hacket-Pain, A., Esper, J., Serrano-Notivoli, R., Hartl, C., Weigel, R., Klesse, S., Resco de Dios, V., Scharnweber, T., Dorado-Liñán, I., van der Maaten-Theunissen, M., van der Maaten, E., Jump, A., Mikac, S., Banzragch, B.-E., Beck, W., Cavin, L., Claessens, H., Čada, V., Čufar, K., Dulamsuren, C., Gričar, J., Gil-Pelegrín, E., Janda, P., Kazimirovic, M., Kreyling, J., Latte, N., Leuschner, C., Longares, L.A., Menzel, A., Merela, M., Motta, R., Muffler, L., Nola, P., Petritan, A.M., Petritan, I.C., Prislan, P., Rubio-Cuadrado, Á., Rydval, M., Stajić, B., Svoboda, M., Toromani, E., Trotsiuk, V., Wilmking, M., Zlatanov, T., de Luis, M., 2022. Climate-change-driven growth decline of European beech forests. Commun. Biol. 5, 1–9. https://doi.org/10.1038/s42003-022-03107-3.

Mausolf, K., Wilm, P., Härdtle, W., Jansen, K., Schuldt, B., Sturm, K., von Oheimb, G., Hertel, D., Leuschner, C., Fichtner, A., 2018. Higher drought sensitivity of radial growth of European beech in managed than in unmanaged forests. Sci. Total Environ. 642, 1201–1208. https://doi.org/10.1016/j.scitotenv.2018.06.065.

McDowell, N.G., Allen, C.D., 2015. Darcy's law predicts widespread forest mortality under climate warming. Nat. Clim. Chang. 5, 669–672. https://doi.org/10.1038/nclimate2641.

McDowell, N.G., Ryan, M.G., Zeppel, M.J.B., Tissue, D.T., 2013. Feature: improving our knowledge of drought-induced forest mortality through experiments, observations, and modeling. New Phytol. 200, 289–293. https://doi.org/10.1111/nph.12502.

Meier, M., Vitasse, Y., Bugmann, H., Bigler, C., 2021. Phenological shifts induced by climate change amplify drought for broad-leaved trees at low elevations in Switzerland. Agric. For. Meteorol. 307, 108485. https://doi.org/10.1016/j.agrformet.2021.108485.

Meusburger, K., Trotsiuk, V., Schmidt-Walter, P., Baltensweiler, A., Brun, P., Bernhard, F., Gharun, M., Habel, R., Hagedorn, F., Köchli, R., Psomas, A., Puhlmann, H., Thimonier, A., Waldner, P., Zimmermann, S., Walthert, L., 2022. Soil–plant interactions modulated water availability of Swiss forests during the 2015 and 2018 droughts. Glob. Change Biol. https://doi.org/10.1111/gcb.16332 n/a.

Meyer, P., Spînu, A.P., Mölder, A., Bauhus, J., 2022. Management alters drought-induced mortality patterns in European beech (*Fagus sylvatica* L.) forests. Plant Biol. https://doi.org/10.1111/plb.13396 n/a.

Monserud, R.A., Sterba, H., 1999. Modeling individual tree mortality for Austrian forest species. For. Ecol. Manag. 113, 109–123. https://doi.org/10.1016/S0378-1127(98)00419-8.

Moravec, V., Markonis, Y., Rakovec, O., Svoboda, M., Trnka, M., Kumar, R., Hanel, M., 2021. Europe under multi-year droughts: how severe was the 2014–2018 drought period? Environ. Res. Lett. 16, 034062. https://doi.org/10.1088/1748-9326/abe828.

Nuske, R., 2021. Vegperiod: Determine Thermal Vegetation Periods. https://doi.org/10.5281/zenodo.4494600.

Nussbaumer, A., Gessler, A., Benham, S., de Cinti, B., Etzold, S., Ingerslev, M., Jacob, F., Lebourgeois, F., Levanic, T., Marjanović, H., Nicolas, M., Ostrogović Sever, M.Z., Priwitzer, T., Rautio, P., Roskams, P., Sanders, T.G.M., Schmitt, M., Šrámek, V., Thimonier, A., Ukonmaanaho, L., Verstraeten, A., Vesterdal, L., Wagner, M., Waldner, P., Rigling, A., 2021. Contrasting resource dynamics in mast years for European beech and oak—a continental scale analysis. Front. For. Glob. Chang. 4, 689836. https://doi.org/10.3389/ffgc.2021.689836.

Pan, Y., Birdsey, R.A., Fang, J., Houghton, R., Kauppi, P.E., Kurz, W.A., Phillips, O.L., Shvidenko, A., Lewis, S.L., Canadell, J.G., Ciais, P., Jackson, R.B., Pacala, S.W., McGuire, A.D., Piao, S., Rautiainen, A., Sitch, S., Hayes, D., 2011. A large and persistent carbon sink in the world's forests. Science 333, 988–993. https://doi.org/10.1126/science.1201609.

Puhlmann, H., von Wilpert, K., 2011. Test und Entwicklung von Pedotransferfunktionen für Wasserretention und hydraulische Leitfähigkeit von Waldböden. Waldökologie Landschaftsforschung Naturschutz 12, 61–71.

R Core Team, 2021. R: A Language and Environment for Statistical Computing.

Rabbel, I., Neuwirth, B., Bogena, H., Diekkrüger, B., 2018. Exploring the growth response of Norway spruce (*Picea abies*) along a small-scale gradient of soil water supply. Dendrochronologia 52, 123–130. https://doi.org/10.1016/j.dendro.2018.10.007.

Rathgeb, U., Bürgi, M., Wohlgemuth, T., 2020. Waldschäden wegen Dürre von 1864 bis 2018 in der Schweiz und insbesondere im Kanton Zürich. Schweiz. Z. Forstwes. 171, 249–256. https://doi.org/10.3188/szf.2020.0249.

Rigling, A., Bräker, O., Schneiter, G., Schweingruber, F., 2002. Intra-annual tree-ring parameters indicating differences in drought stress of *Pinus sylvestris* forests within the Erico-pinion in the Valais (Switzerland). Plant Ecol. 163, 105–121. https://doi.org/10.1023/A:1020355407821.

Rigling, A., Bigler, C., Eilmann, B., Feldmeyer-Christe, E., Gimmi, U., Ginzler, C., Graf, U., Mayer, P., Vacchiano, G., Weber, P., Wohlgemuth, T., Zweifel, R., Dobbertin, M., 2013. Driving factors of a vegetation shift from scots pine to pubescent oak in dry alpine forests. Glob. Chang. Biol. 19, 229–240. https://doi.org/10.1111/gcb.12038.

Ripullone, F., Camarero, J.J., Colangelo, M., Voltas, J., 2020. Variation in the access to deep soil water pools explains tree-to-tree differences in drought-triggered dieback of Mediterranean oaks. Tree Physiol. 40, 591–604. https://doi.org/10.1093/treephys/tpaa026.

Roberts, J., Cabral, O.M.R., De Aguiar, L.F., 1990. Stomatal and boundary-layer conductances in an Amazonian terra Firme rain forest. J. Appl. Ecol. 27, 336–353. https://doi.org/10.2307/2403590.

Rohner, B., Kumar, S., Liechti, K., Gessler, A., Ferretti, M., 2021. Tree vitality indicators revealed a rapid response of beech forests to the 2018 drought. Ecol. Indic. 120, 106903. https://doi.org/10.1016/j.ecolind.2020.106903.

Ryan, M.G., Yoder, B.J., 1997. Hydraulic limits to tree height and tree growth. Bioscience 47, 235–242. https://doi.org/10.2307/1313077.

Salomón, R.L., Peters, R.L., Zweifel, R., Sass-Klaassen, U.G.W., Stegehuis, A.I., Smiljanic, M., Poyatos, R., Babst, F., Cienciala, E., Fonti, P., Lerink, B.J.W., Lindner, M., Martinez-Vilalta, J., Mencuccini, M., Nabuurs, G.-J., van der Maaten, E., von Arx, G., Bär, A., Akhmetzyanov, L., Balanzategui, D., Bellan, M., Bendix, J., Berveiller, D., Blaženec, M., Čada, V., Carraro, V., Cecchini, S., Chan, T., Conedera, M., Delpierre, N., Delzon, S., Ditmarová, Ľ., Dolezal, J., Dufrêne, E., Edvardsson, J., Ehekircher, S., Forner, A., Frouz, J., Ganthaler, A., Gryc, V., Güney, A., Heinrich, I., Hentschel, R., Janda, P., Ježík, M., Kahle, H.-P., Knüsel, S., Krejza, J., Kuberski, Ł., Kučera, J., Lebourgeois, F., Mikoláš, M., Matula, R., Mayr, S., Oberhuber, W., Obojes, N., Osborne, B., Paljakka, T., Plichta, R., Rabbel, I., Rathgeber, C.B.K., Salmon, Y., Saunders, M., Scharnweber, T., Sitková, Z., Stangler, D.F., Stereńczak, K., Stojanović, M., Střelcová, K., Světlík, J., Svoboda, M., Tobin, B., Trotsiuk, V., Urban, J., Valladares, F., Vavrčík, H., Vejpustková, M., Walthert, L., Wilmking, M., Zin, E., Zou, J., Steppe, K., 2022. The 2018 European heatwave led to stem dehydration but not to consistent growth reductions in forests. Nat. Commun. 13, 28. https://doi.org/10.1038/s41467-021-27579-9.

Schmidt-Walter, P., Trotsiuk, V., Meusburger, K., Zacios, M., Meesenburg, H., 2020. Advancing simulations of water fluxes, soil moisture and drought stress by using the LWF-Brook90 hydrological model in R. Agric. For. Meteorol. 291, 108023. https://doi.org/10.1016/j.agrformet.2020.108023.

Schuldt, B., Buras, A., Arend, M., Vitasse, Y., Beierkuhnlein, C., Damm, A., Gharun, M., Grams, T.E.E., Hauck, M., Hajek, P., Hartmann, H., Hiltbrunner, E., Hoch, G., Holloway-Phillips, M., Körner, C., Larysch, E., Lübbe, T., Nelson, D.B., Rammig, A., Rigling, A., Rose, L., Ruehr, N.K., Schumann, K., Weiser, F., Werner, C., Wohlgemuth, T., Zang, C.S., Kahmen, A., 2020. A first assessment of the impact of the extreme 2018 summer drought on central European forests. Basic Appl. Ecol. 45, 86–103. https://doi.org/10.1016/j.baae.2020.04.003.

Skippy, 2022. WSL [WWW Document]. https://www.wsl.ch/de/services-und-produkte/forschungsinstrumente/skippy.html.

Sohn, J.A., Saha, S., Bauhus, J., 2016. Potential of forest thinning to mitigate drought stress: a meta-analysis. For. Ecol. Manag. 380, 261–273. https://doi.org/10.1016/j.foreco.2016.07.046.

Stojnić, S., Suchocka, M., Benito-Garzón, M., Torres-Ruiz, J.M., Cochard, H., Bolte, A., Cocozza, C., Cvjetković, B., de Luis, M., Martinez-Vilalta, J., Ræbild, A., Tognetti, R., Delzon, S., 2018. Variation in xylem vulnerability to embolism in European beech from geographically marginal populations. Tree Physiol. 38, 173–185. https://doi.org/10.1093/treephys/tpx128.

Stovall, A.E.L., Shugart, H., Yang, X., 2019. Tree height explains mortality risk during an intense drought. Nat. Commun. 10, 4385. https://doi.org/10.1038/s41467-019-12380-6.

Sturm, J., Santos, M.J., Schmid, B., Damm, A., 2022. Satellite data reveal differential responses of Swiss forests to unprecedented 2018 drought. Glob. Change Biol. https://doi.org/10.1111/gcb.16136.

Tejedor, E., Serrano-Notivoli, R., de Luis, M., Saz, M.A., Hartl, C., St. George, S., Büntgen, U., Liebhold, A.M., Vuille, M., Esper, J., 2020. A global perspective on the climate-driven growth synchrony of neighbouring trees. Glob. Ecol. Biogeogr. 29, 1114–1125. https://doi.org/10.1111/geb.13090.

Thornton, P.E., Running, S.W., White, M.A., 1997. Generating surfaces of daily meteorological variables over large regions of complex terrain. J. Hydrol. 190, 214–251. https://doi.org/10.1016/S0022-1694(96)03128-9.

Trotsiuk, V., Hartig, F., Cailleret, M., Babst, F., Forrester, D.I., Baltensweiler, A., Buchmann, N., Bugmann, H., Gessler, A., Gharun, M., Minunno, F., Rigling, A., Rohner, B., Stillhard, J., Thürig, E., Waldner, P., Ferretti, M., Eugster, W., Schaub, M., 2020. Assessing the response of forest productivity to climate extremes in Switzerland using model–data fusion. Glob. Chang. Biol. 26, 2463–2476. https://doi.org/10.1111/gcb.15011.

Trugman, A.T., Anderegg, L.D.L., Anderegg, W.R.L., Das, A.J., Stephenson, N.L., 2021. Why is tree drought mortality so hard to predict? Trends Ecol. Evol. 36, 520–532. https://doi.org/10.1016/j.tree.2021.02.001.

Trumbore, S., Brando, P., Hartmann, H., 2015. Forest health and global change. Science 349, 814–818. https://doi.org/10.1126/science.aac6759.

Voltas, J., Camarero, J.J., Carulla, D., Aguilera, M., Ortiz, A., Ferrio, J.P., 2013. A retrospective, dual-isotope approach reveals individual predispositions to winter-drought induced tree dieback in the southernmost distribution limit of Scots pine. Plant Cell Environ. 36, 1435–1448. https://doi.org/10.1111/pce.12072.

Walthert, L., Ganthaler, A., Mayr, S., Saurer, M., Waldner, P., Walser, M., Zweifel, R., von Arx, G., 2021. From the comfort zone to crown dieback: sequence of physiological stress

thresholds in mature European beech trees across progressive drought. Sci. Total Environ. 753, 141792. https://doi.org/10.1016/j.scitotenv.2020.141792.
Wohlgemuth, T., Kistler, M., Aymon, C., Hagedorn, F., Gessler, A., Gossner, M.M., Queloz, V., Vögtli, I., Wasem, U., Vitasse, Y., Rigling, A., 2020. Früher Laubfall der Buche während der Sommertrockenheit 2018: Resistenz oder Schwächesymptom? Schweiz. Z. Forstwes. 171, 257–269. https://doi.org/10.3188/szf.2020.0257.
Young, D.J.N., Stevens, J.T., Earles, J.M., Moore, J., Ellis, A., Jirka, A.L., Latimer, A.M., 2017. Long-term climate and competition explain forest mortality patterns under extreme drought. Ecol. Lett. 20, 78–86. https://doi.org/10.1111/ele.12711.
Zweifel, R., Ginzler, C., Psomas, A., Braun, S., Walthert, L., Etzold, S., 2020. Baumwasserdefizite erreichten im Sommer 2018 Höchstwerte – war das aus dem All erkennbar? Schweiz. Z. Forstwes. 171, 302–305. https://doi.org/10.3188/szf.2020.0298.